Title

Tailoring hydrogel surface properties to modulate cellular response to shear loading

Authors

Meinert, Christoph
Schrobback, Karsten
Levett, Peter A
et al.

Publication Date

2017-04-01

DOI

10.1016/j.actbio.2016.10.011

Peer reviewed

HHS Public Access

Author manuscript

Acta Biomater. Author manuscript; available in PMC 2018 April 01.

Published in final edited form as:

Acta Biomater. 2017 April 01; 52: 105–117. doi:10.1016/j.actbio.2016.10.011.

Tailoring hydrogel surface properties to modulate cellular response to shear loading

Christoph Meinert[1], **Karsten Schrobback**[1], **Peter A. Levett**[1], **Cameron Lutton**[1], **Robert L. Sah**[2], and **Travis J. Klein**[1,*]

[1]Institute of Health and Biomedical Innovation, Queensland University of Technology, Brisbane, Queensland, 4059, Australia

[2]Department of Bioengineering, University of California-San Diego, La Jolla, California, 92093, United States of America

Abstract

Biological tissues at articulating surfaces, such as articular cartilage, typically have remarkable low-friction properties that limit tissue shear during movement. However, these frictional properties change with trauma, aging, and disease, resulting in an altered mechanical state within the tissues. Yet, it remains unclear how these surface changes affect the behaviour of embedded cells when the tissue is mechanically loaded. Here, we developed a cytocompatible, bilayered hydrogel system that permits control of surface frictional properties without affecting other bulk physicochemical characteristics such as compressive modulus, mass swelling ratio, and water content. This hydrogel system was applied to investigate the effect of variations in surface friction on the biological response of human articular chondrocytes to shear loading. Shear strain in these hydrogels during dynamic shear loading was significantly higher in high-friction hydrogels than in low-friction hydrogels. Chondrogenesis was promoted following dynamic shear stimulation in chondrocyte-encapsulated low-friction hydrogel constructs, whereas matrix synthesis was impaired in high-friction constructs, which instead exhibited increased catabolism. Our findings demonstrate that the surface friction of tissue-engineered cartilage may act as a potent regulator of cellular homeostasis by governing the magnitude of shear deformation during mechanical loading, suggesting a similar relationship may also exist for native articular cartilage.

Graphical Abstract

[*]**Corresponding author:** Travis J. Klein, PhD, Institute of Health and Biomedical Innovation, Queensland University of Technology, 60 Musk Avenue, Kelvin Grove, Queensland 4059, Australia, t2.klein@qut.edu.au, Phone: +61 7 3138 6142, Fax: +61 7 3138 6030.

Competing financial interests

The authors declare no competing financial interest.

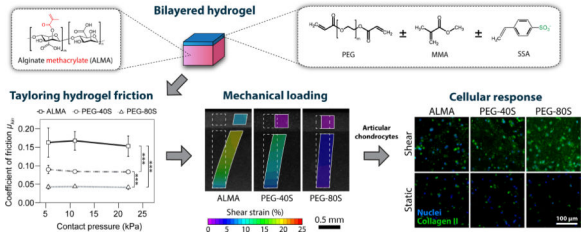

1. Introduction

Hydrogels are highly-hydrated three-dimensional (3D) matrices formed of crosslinked polymeric networks which show promise in a variety of biomedical applications including medical devices, drug delivery, and as scaffolds for tissue engineering and regenerative medicine [1]. Hydrogels allow for cell encapsulation with high viability [2], can be readily tuned to mimic key features of the native extracellular matrix (ECM) [3, 4], permit control of mechanical and physicochemical properties [5], and facilitate physiological cell differentiation and function [6]. Additionally, their surface friction can be tailored by manipulating the gel's chemical structure, hydrophilicity, crosslinking density, water content, elasticity, or charge density [7]. As such, they offer key advantages over traditional, two-dimensional cell culture methods which frequently fail to adequately mimic the extracellular microenvironment associated with physiological tissue and disease-associated processes [8]. As a result, the use of hydrogels as engineered microenvironments to study cellular behaviour in a more physiologically relevant manner has been increasing steadily [9]. Previous studies using hydrogels as ECM mimics emphasized the role of the structural and mechanical properties of the cellular microenvironment, in particular ECM stiffness, which has been shown to affect cell motility [10], stem cell differentiation [11–13], tumour progression [14], cellular reprogramming [15], and other biological phenomena. However, it remains largely unclear how these and other physicochemical ECM properties impact cellular behaviour when the tissue is loaded mechanically.

Most mammalian cell types including chondrocytes, the cells within cartilage, respond to mechanical stimuli through mechanotransduction - a process by which cells convert physical forces to biochemical signals [16]. While mechanical stress within a certain, physiological range induces anabolic processes and thus contributes to cartilage ECM maintenance and remodelling [17, 18], excessive stress is considered to be a main driving factor for catabolic processes initiating joint pathology and degeneration in diseases such as osteoarthritis (OA) [19, 20]. To prevent excessive tissue strains during joint ambulation, healthy synovial joints exhibit remarkably effective lubrication [21–25] leading to a coefficient of friction (COF) as low as 0.001 – 0.025 for cartilage-on-cartilage – a value lower than any other known bearing [26–29]. Given these extremely low COFs, shear strains resulting from normal joint articulation are minor and may have a rather protective function on cartilage homeostasis, inducing extracellular matrix production and turnover [30, 31]. Acute injury, changes in biomechanics, or inflammatory events, however, result in a reduced lubricating function and increased frictional forces between articulating surfaces [32–35]. This may in turn be involved in the initiation of posttraumatic cartilage degeneration by increasing the

magnitude of loading-induced tissue strain beyond a physiological level. Nevertheless, although earlier studies suggested an increase in shear strain following superficial cartilage damage and depleted lubrication [36–38], surprisingly little is known about the functional relationship between the frictional properties of native or tissue-engineered cartilage and chondrocyte behaviour upon mechanical stimulation.

In this work, we aimed to harness the adaptability of hydrogel materials to investigate the role of variations in surface friction on the biological response of articular chondrocytes to physiologically relevant mechanical stimulation. We, therefore, established and characterized a poly(ethylene glycol) diacrylate (PEG)-based hydrogel system that allows for tailoring of the COF to model the frictional properties of healthy, damaged, and osteoarthritic cartilage. Thin sheets of these hydrogels were then co-polymerized with chondrocyte-laden, photocrosslinkable alginate methacrylate (ALMA), which supports a chondrogenic cell phenotype [39], to form bilayered hydrogel constructs with tuneable surface friction. Constructs containing human articular chondrocytes were finally subjected to dynamic shear loading in a customized mechanical stimulation bioreactor to investigate the effects of variations in surface friction on the phenotypic expressions of encapsulated chondrocytes.

2. Materials and methods

2.1. Synthesis of Alginate Methacrylate (ALMA)

Medium viscosity alginate (MW ~ 260 kDa) was modified to include photocrosslinkable groups by reaction with methacrylic anhydride (MAAh) (both Sigma-Aldrich, St Louis, MO, USA). Alginate was dissolved in distilled water at 2 % and reacted with a 10-fold molar excess of MAAh over total alginate hydroxyl groups for 24 h on ice and under constant stirring [40]. The pH was regularly adjusted to 8 using 5 M NaOH. After the reaction period, insoluble MAAh was removed by centrifugation, followed by dialysis against deionized water using a 12 kDa MWCO cellulose dialysis membrane (Sigma-Aldrich) for 5–7 days. The pH of the dialyzed polymer solutions was adjusted to 7.4, after which they were lyophilized and stored at −20 °C protected from light and moisture.

2.2. Chondrocyte Isolation and Expansion Culture

Articular cartilage was obtained with institutional ethics approval from consenting patients undergoing total knee replacement surgeries for osteoarthritis (donors: two female + one male, age 62 – 80 years). Chondrocytes were isolated from areas of macroscopically normal full-thickness cartilage, as described elsewhere [41]. Cells were propagated on tissue culture plastic (3000 cells/cm^2) in low-D-glucose chondrocyte basal medium (Dulbecco's modified Eagle's medium (DMEM) with 2 mM GlutaMAX™, 10 mM 4-(2-hydroxyethyl)-1-piperazineethanesulfonic acid (HEPES), 0.1 mM nonessential amino acids, 50 U/mL penicillin, 50 μg/mL streptomycin, 0.5 μg/mL amphotericin B (Fungizone®) (all Invitrogen, CA, USA), 0.4 mM L-proline and 0.1 mM L-ascorbic acid (both Sigma-Aldrich)) supplemented with 10 % foetal bovine serum (FBS) (Hyclone, Logan, UT, USA).

Unless stated otherwise, all cells and cell/hydrogel constructs were maintained at 37 °C in a humidified 5 % CO_2/95 % air CO_2 incubator with the medium refreshed every 3–4 days.

2.3. Preparation of Thin Hydrogel Sheets with Controlled Frictional Properties

To tailor the frictional properties of poly(ethylene glycol) diacrylate-based hydrogels (PEG, average M_n = 700 g/mol), various concentrations of negatively charged 4-styrene sulfonic acid (SSA) (both Sigma-Aldrich) were added to the PEG precursor solution and covalently incorporated into the PEG network during photo-polymerization. In order to retain alike total molarities and comparable polymer network densities in all PEG-based hydrogels, the uncharged compound methyl methacrylate (MMA) was added to hydrogels with a lower SSA content (PEG-40S) (Table 1). Just like SSA, MMA allows photocrosslinking via its vinyl group, resulting in comparable crosslinking densities.

Briefly, 2 % w/v ALMA or PEG/SSA with or without MMA were dissolved in phosphate-buffered saline (PBS) containing 0.2 % w/v Irgacure 2959 (1-(4-(2-hydroxyethoxy)-phenyl)-2-hydroxy-2-methyl-1-propane-1-one, BASF, Ludwigshafen, Germany) and sterile filtered using a 0.2 μm syringe filter. Hydrogels were photocrosslinked between two parallel glass slides separated with a 300 μm spacer by exposure to 365 nm light at an intensity of ~ 2.5 mW/cm^2 in a CL-1000 crosslinker (UVP, Upland, CA, USA) for 30 minutes. The glass slides were separated after solidification, leaving a thin hydrogel layer behind on one of the slides. Hydrogels were washed briefly in sterile PBS to remove unreacted compounds.

2.4. Cell Encapsulation and Culture

Passage 2 chondrocytes were suspended in 2 % w/v ALMA in PBS containing 0.05 % w/v Irgacure 2959 at a density of 10 million cells/mL. The cell/polymer suspension was then transferred to a custom Teflon casting mold, covered by a glass slide, and initially photocrosslinked for 3 minutes until just solidified. To form bilayered hydrogels with controlled surface friction, the glass slide was removed from the casting mold and replaced by another slide carrying the previously crosslinked PEG-SSA or ALMA hydrogel sheets. The constructs were further polymerized for 9 minutes to ensure proper bonding of the hydrogel layers. Bilayered hydrogel constructs were removed from the casting mold, rinsed with PBS, and cut into constructs with the dimensions of 4 mm × 4 mm × 2 mm using custom cutting guides.

Cell/hydrogel constructs were cultured in serum-free high-D-glucose basal chondrocyte medium (see above for composition) with ITS-G (100 × dilution), 1.25 mg/mL bovine serum albumin (BSA), 0.1 μM dexamethasone (all Sigma-Aldrich) and 10 ng/mL transforming growth factor beta 3 (TGF-β3) (GroPep, Adelaide, SA, Australia), and this media was also used as a lubricant in mechanical stimulation experiments.

2.5. Mechanical Stimulation

Dynamic shear stimulation was carried out in a custom bioreactor chamber (Fig. 1D) mounted to a commercially available displacement-controlled mechanical loading bioreactor (Cartigen C10-12c, Tissue Growth Technologies, Minnetonka, MN, USA). The chamber translates the vertical movement of the bioreactor actuator to horizontal movement of two

loading platens manufactured from non-porous stainless steel (Supplementary Video V1), each platen stimulating up to 8 cell/hydrogel constructs simultaneously without physical contact between the samples. The displacement of the platens is not affected by the surface properties of the hydrogel constructs, but the dynamic shear strain within the hydrogel depends on the hydrogel frictional properties (Figure 2F, G). The chamber was designed to apply an offset compression of ~ 15 % of the construct height to all dynamically stimulated constructs and static controls. The bioreactor was placed in a humidified 5 % CO_2/95 % air CO_2 incubator. Sterile gas exchange was assured through a syringe filter unit with 0.2 μm pore size mounted onto the bioreactor chamber.

Gene expression analysis following short-term mechanical stimulation was performed to determine a suitable shear loading amplitude for long-term loading experiments. Cell/hydrogel constructs were precultured for 7 days under free-swelling conditions to allow for chondrocyte redifferentiation and formation of a protective pericellular matrix [42] prior to mechanical stimulation. Constructs were then dynamically stimulated for 1 h at 1 Hz and either 0 mm (static control), 0.15 mm, 0.315 mm, or 1 mm shear loading amplitude (Fig. 1E). Long-term experiments were performed to determine the effects of variations in surface friction on construct biomechanical properties, ECM accumulation, and chondrocyte gene expression in response to intermittent shear loading. Constructs were precultured under free-swelling conditions for 21 days, followed by intermittent shear stimulation for the next 11 days at 1 mm displacement amplitude and a frequency of 1 Hz for 1 h daily (Fig. 1F). Since our previous experiments suggested that mRNA levels peak at 2 hours post-completion of mechanical loading [42], constructs were terminated for qRT-PCR 2 hours after the final shear stimulation cycle had ceased.

2.6. Hydrogel Frictional Properties

Measurement of hydrogel surface friction was performed using a custom reciprocating tribometer that enables control of normal force (F_N) and lubricant temperature. The tribometer was attached to an Instron 5848 microtester configured horizontally with a 5 N load cell (Instron, Melbourne, VIC, Australia). Hydrogels were fixed to the apparatus with epoxy adhesive (Loctite, Henkel, Duesseldorf, Germany) without compromising the gel surface. Defined normal forces of 88 mN, 176 mN, and 352 mN were applied onto the hydrogel constructs resulting in contact pressures of 5.5 kPa, 11 kPa, and 22 kPa, respectively. Frictional forces against the loading platen of the shear loading bioreactor (stainless steel) were assessed over a sliding distance of 10 mm for 5 reciprocating cycles at a constant sliding velocity of 1 mm/s in high-D-glucose basal chondrocyte medium with ITS-G (100 × dilution) and 1.25 mg/mL BSA. The dynamic coefficient of friction (COF) was calculated for each sample based on the average measured frictional forces (F_f) and the applied F_N using the equation $COF = F_f / F_N$.

2.7. Hydrogel Physical Properties

The compressive moduli of bilayered hydrogel constructs were measured in an unconfined arrangement using an Instron 5848 microtester with a 5 N load cell (Instron). During testing constructs were submerged in PBS at 37 °C. A displacement rate of 0.01 mm/s was applied using a non-porous indenter, and the modulus was taken from the linear region of the stress–

strain curve from 10 % to 15 % strain [5]. The mass swelling ratio was determined by the ratio of equilibrium wet weight of swollen gels to dry weight of lyophilized gels.

2.8. EPIC-μCT

The distribution of fixed negative charges in bilayered hydrogel constructs was visualized using equilibrium partitioning of an ionic contrast agent microcomputed tomography (EPIC-μCT) [43]. Constructs were incubated overnight in a mixture of 40 % ioxaglate (Hexabrix; Aspen, St Leonards, NSW, Australia) in PBS at room temperature on a shaker plate. Constructs were then imaged in a μCT 40 scanner (Scanco Medical, Brüttisellen, Switzerland) at 45 kV and 177 μA with a 12 μm isotropic voxel size. Images were analyzed using Scanco μCT software and ImageJ (National Institutes of Health, USA).

2.9. Micro-Scale Shear Testing and Digital Image Correlation

Bilayered ALMA, PEG-40S, and PEG-80S hydrogels containing Fluoresbrite® fluorescent microspheres (Polysciences, Taipei, Taiwan; 10 million microspheres/mL in 2% (w/v) ALMA layer, 20 million microspheres/mL in variable friction surface layer) were prepared as above (cell-free) and incubated in PBS overnight. A custom microscope-mounted mechanical loading system capable of applying precise compressive and shear stimulation facilitated by a stainless steel loading platen was employed to apply sliding shear motion to hydrogel constructs. Testing was performed submerged in PBS at a sliding velocity of 0.1 mm/s (~ 15 % offset compressive strain). Hydrogel shear strains in the variable friction and ALMA layer, respectively, were determined using Vic-2D digital image correlation software (Correlated Solutions, Columbia, SC, USA; Step size: 20, subset size: 81).

2.10. Viability Assay

Live and dead cells were visualized with fluorescein diacetate (FDA) and propidium iodide (PI) (both Sigma-Aldrich), respectively. Hydrogel constructs were washed in PBS, incubated in a solution of 10 μg/mL FDA and 5 μg/mL PI in PBS for 5 min at 37 °C, and then washed twice in PBS. Images were captured using a Nikon Eclipse fluorescence microscope.

2.11. Gene Expression Analysis

Hydrogel constructs were homogenized in 1 mL of TRIzol reagent (Invitrogen), and total RNA was isolated according to the manufacturer's instructions. SuperScript™ III First Strand Synthesis System (Invitrogen) was used to synthesize complementary DNA (cDNA). DNase and RNase digestions were performed before and after cDNA synthesis, respectively. Quantitative real-time polymerase chain reaction (qRT-PCR) was carried out using SybrGreen® Mastermix (Invitrogen) and a 7900HT fast real-time PCR system (Applied Biosystems). The cycle threshold (C_t) value of each gene was normalized to the geometric mean of the housekeeping genes *RPL13A* and *B2M* using the comparative C_t method ($2^{-\Delta Ct}$). Primer sequences were used as published previously (*COL1A1* [44], *COL2A1* [44], *ACAN* [44], *PRG4* [44], *RPL13A* [45] and *B2M* [45]). Primers for *MMP3* were purchased from Qiagen (Venlo, Netherlands).

2.12. Immunofluorescence Analysis

Constructs were frozen in Optimal Cutting Temperature compound (OCT) (Sakura, Finetek, Tokyo, Japan) and sectioned at a thickness of 10 μm. Sections were fixed with ice-cold acetone, air-dried, and rehydrated in 50 mM $BaCl_2$/100 mM Tris HCL buffer (pH 7.3) for 1 h, followed by incubation with 100 mM Tris HCL buffer (pH 7.3) for 5 min. Antigen retrieval with 0.1 % hyaluronidase (Sigma-Aldrich) at 37 °C for 30 minutes was performed on sections to be stained for collagen type I and collagen type II. Primary antibodies for aggrecan (969D4D11, Invitrogen; 1:400 dilution in PBS with 2 % donkey serum), collagen type I (I-8H5, MP Biomed, Solon, OH, USA; 1:300 dilution in PBS with 2 % goat serum), and collagen type II (II-II6B3, Developmental Studies Hybridoma Bank (DSHB), Iowa City, IA, USA; 1:100 dilution in PBS with 2 % goat serum) were applied in a humidified chamber at 4 °C overnight. Secondary antibodies were diluted 1:150 in PBS with 2 % goat/donkey serum and 5 μg/mL 4′,6-diamidino-2-phenylindole (DAPI) (Invitrogen) and applied for 1 h in the dark (AlexaFluor® 488-labelled donkey anti-mouse, AlexaFluor® 488-labelled goat antimouse, AlexaFluor® 594-labelled goat anti-mouse; all Jackson ImmunoResearch, West Grove, PA, USA). A mouse IgG isotype control antibody (Jackson ImmunoResearch; 1:1000 dilution) and secondary antibody only were used as negative controls. After two washing steps in PBS and drying, sections were mounted with ProLong Gold (Invitrogen) and imaged using a Zeiss Axio microscope.

Integrated fluorescence intensities of histological sections were calculated using ImageJ software (National Institutes of Health, USA) and normalized to the integrated fluorescence intensity of DAPI stainings in order to correct the obtained values for differences in cell numbers between microscopic images.

2.13. Biochemical Analysis

To quantify retained glycosaminoglycans (GAG) and DNA, cultured constructs were frozen and lyophilized. After careful removal of the cell-free surface hydrogel layer, the cell-laden proportions of the constructs were digested overnight in 0.5 mg/mL proteinase K (Invitrogen) at 56 °C on an Eppendorf® Thermomixer® (Eppendorf, Hamburg, Germany). GAG concentration in the digest was measured using the dimethyl-methylene blue (DMMB) assay (pH 1.5). Absorbances at 525 and 595 nm were measured, and concentrations calculated using the ratio of absorbances, compared to a quadratic standard curve prepared from chondroitin sulfate C (Sigma-Aldrich). DNA concentrations in the digests were measured using the Quant-iT™ PicoGreen® dsDNA quantification assay (Invitrogen).

2.14. Statistical Analysis

Statistical analyses were performed using SPSS software (version 20, IBM Corporation, USA). Differences between groups were determined using analysis of variance (ANOVA) and Tukey's or Dunnet's T3 post-hoc tests as appropriate, with a significance level of 0.05. Statistically significant differences are indicated in figures using symbols.

3. Results

3.1. Tailoring hydrogel surface friction

We established a PEG-based hydrogel system which allows for control of its frictional properties by varying the density of fixed negative charge facilitated by 4-styrene-sulfonic acid (SSA) (Fig. 1B, C) to mimic the increase in articular cartilage surface friction following damage and degeneration [46]. To accomplish this, three separate compositions were prepared to yield thin hydrogel sheets containing no SSA (alginate methacrylate, or ALMA; Fig. 1A), 40 mol% SSA (PEG-40S), or 80 mol% SSA (PEG-80S), respectively. The obtained hydrogels sheets were then combined with a layer of ALMA containing human articular chondrocytes to form bilayered hydrogel constructs by photopolymerization. ALMA, which was synthesized by reaction of alginate with methacrylic anhydride, allows for polymerization in the presence of a photoinitiator and light under physiological conditions, allowing *in situ* crosslinking and cell encapsulation with high cell viabilities (Fig. 1A) [39].

The frictional properties of hydrogel constructs were assessed against the stainless steel loading platen of the shear bioreactor used in the following experiments using cell culture media as lubricant. For PEG-80S constructs, we observed kinetic COFs of ~ 0.045 for all investigated normal pressures (Fig. 2A), values that approximate to previously reported COFs of healthy cartilage-on-cartilage (0.001 – 0.025) [26–29]. PEG-40S and ALMA hydrogels exhibited significantly higher COFs ranging from ~ 0.085 to ~ 0.092, and ~ 0.155 to ~ 0.170, respectively. The latter values correspond to COFs previously reported for cartilage affected by moderate to severe OA (stage 3–4; Fig. 2A) [27, 46, 47]. EPIC-μCT scans were performed to confirm that the variations in construct surface friction were indeed associated with differences in the distribution and concentration of fixed negative charges. Due to the repulsion of the anionic contrast agent ioxaglate, μCT attenuation levels in the variable friction layer were reduced with increasing concentration of negatively charged SSA (Fig. 2D, E) which resulted in a significant change of construct surface friction (Fig. 2A, $p < 0.001$).

We then proceeded to investigate the deformation of these constructs in response to sliding shear motion replicating the mechanical environment of articular cartilage using a custom microscope-mounted loading device and digital image correlation. Similar to native articular cartilage [37, 38], deformation of the hydrogel constructs was highly dependent on their surface friction (Fig. 2F, G). When applying shear stimulation, initially the construct surfaces adhered to the loading platen and began to displace laterally, causing depth-diminishing shear deformation of the cell-laden hydrogels which peaked just below the surface hydrogel layer. With further displacement, the construct surfaces detached and slid relative to the loading platen with a steady-state peak strain. The magnitude of this strain was dependent on the surface friction of the constructs with strain magnitudes increasing with higher construct COFs (Fig. 2F, G). Changes in the composition of the surface hydrogel layer had no measurable effect on the bulk compressive moduli (Fig. 2B), the mass swelling ratio, or the water content (Fig. 2C) of bilayered constructs which remained statistically similar between construct types.

3.2. Effects of short-term mechanical stimulation on chondrocyte viability and gene expression

Short- and long-term dynamic shear stimulation (Fig. 1E, F) was carried out in a custom bioreactor chamber (Fig. 1D and Supplementary Video V1) to assess the effects of differences in construct surface friction on the biological response of encapsulated chondrocytes. In order to investigate whether cell viability was affected by dynamic loading, we performed fluorescein diacetate/propidium iodide stainings 24 hours after mechanical loading had ceased to allow cells to undergo necrotic or programmed cell death. Hydrogel-encapsulated human articular chondrocytes exhibited round cell morphologies indicative of a chondrogenic phenotype [48] and high cell viabilities (> 90%) were observed in all construct types in both shear-stimulated and static controls, suggesting that neither the hydrogel composition nor mechanical loading had cytotoxic effects (Fig. 3). To determine the optimal shear loading amplitude for chondrocyte culture, constructs were dynamically stimulated at various shear amplitudes (0.15 mm, 0.315 mm, 1 mm) in a short-term experiment and changes in gene expression levels were assessed using qRT-PCR (Fig. 4). Among the investigated amplitudes, dynamic stimulation at 1 mm loading plate extension led to differential regulation of the investigated genes (Supplementary Fig. S1), and this amplitude was chosen for the following long-term experiments.

3.3. Effects of surface friction on chondrocyte gene expression and construct properties in long-term shear-stimulated hydrogel cultures

Key biochemical features of articular cartilage include the abundant presence of collagen type II and proteoglycans which interact with a fluid environment to provide the tissue with its unique biomechanical properties [49]. The expression of genes including *COL2A1* encoding the alpha chain of collagen type II, *ACAN* encoding the proteoglycan aggrecan, and *PRG4* encoding the superficial zone-specific boundary lubricant proteoglycan 4 (PRG4) are thus commonly used as markers of the chondrogenic phenotype. When the expression of these genes was investigated after long-term intermittent shear stimulation, we found a distinctive transcriptional response of chondrocytes to mechanical stimuli which was highly dependent on construct surface friction. While aggrecan transcript levels were comparable between all groups (Fig. 4A), we found ~ 15.8-fold higher expression of the chondrogenic marker *COL2A1* (Fig. 4B) and ~ 1.8-fold higher expression of *PRG4* (Fig. 4C) in shear-stimulated PEG-80S low friction constructs compared to static controls ($p = 0.005$ for *COL2A1*; $p = 0.041$ for *PRG4*) and ALMA high friction constructs ($p = 0.006$ for *COL2A1*; $p = 0.018$ for *PRG4*). In contrast, expression of chondrogenic marker genes in shear-stimulated ALMA constructs remained at control levels, while expression of the gene encoding matrix metalloproteinase 3 (*MMP3*) was significantly elevated over static controls ($p = 0.032$; Fig. 4E).

Articular cartilage has a high content of glycosaminoglycans (GAGs) which significantly contribute to the compressive stiffness of the tissue and is used as a marker for chondrogenesis [49]. We found that shear stimulation did not affect the GAG/DNA content of ALMA and PEG-40S constructs when compared to statically cultured controls (Fig. 4G). However, mechanically loaded PEG-80S constructs had significantly elevated GAG/DNA levels than their static controls ($p = 0.009$), PEG-40S ($p = 0.001$) and ALMA ($p = 0.012$).

Additionally, intermittent application of dynamic shear also led to increased stiffness of ALMA ($p = 0.036$) and PEG-80S ($p = 0.029$) constructs when compared to unstimulated controls (Fig. 4H). The DNA content after a total of 32 days of culture was similar between all construct types, with or without application of intermittent shear (Fig. 4F), suggesting that mechanical loading did not cause cell death or influence cell proliferation.

To confirm the gene expression data, immunofluorescence analysis was performed to assess the accumulation of cartilaginous matrix proteins and the chondrocyte de-differentiation marker collagen type I in shear-stimulated and statically cultured constructs. While articular cartilage is primarily composed of water, the solid fraction predominantly consists of collagen II and aggrecan. Our results show that aggrecan, collagen type II, and collagen type I immunoreactivity largely confirmed the results observed on mRNA level (Fig. 5). Aggrecan immunostaining was mainly limited to intracellular and pericellular regions and no differences were observed between construct types and shear-stimulated or static control samples (Fig. 5A–F, and S). However, the staining intensity for collagen type II in dynamically stimulated constructs increased markedly with decreasing surface friction and the highest intensities were observed for PEG-80S constructs when compared to PEG-40S ($p < 0.001$) and ALMA ($p < 0.001$; Fig. 5G–L, and T). When compared to static controls, the average fluorescence intensities were higher in PEG-80S ($p < 0.001$), while loaded ALMA constructs exhibited lower intensities than their unstimulated controls ($p = 0.009$) and PEG-40S ($p = 0.011$). No statistically significant differences were observed for the intensity of collagen type I staining, although inter-territorial reactivity appeared stronger in shearstimulated constructs (Fig. 5M–R, and U).

4. Discussion

Articular cartilage is a mechanically-sensitive tissue that can respond favourably or unfavourably to biomechanical stimuli. In healthy diarthrodial joints, nearly friction-less articulation is facilitated by lubricant molecules at the cartilage surface and in synovial fluid including proteoglycan 4 [50], surface active-phospholipids [51], and hyaluronic acid [23], as well as other synergistically interacting lubrication mechanism such as hydrodynamic lubrication and interstitial fluid pressurization [52]. While various pathogenic mechanisms can lead to cartilage deterioration and not necessarily involve elevated surface friction [53], compelling evidence suggests that a loss of the lubricating properties of synovial fluid, often associated with decreased concentrations of proteoglycan 4, results in increased articular surface friction following acute joint injury [32–34, 47, 54–57]. The increase in friction also correlates with the severity of degeneration and osteoarthritis in affected joints [58, 59], suggesting a potential involvement in the pathogenesis of articular cartilage. Interestingly, shear deformation of articular cartilage under mechanical loading is significantly greater with deficient lubrication and pathological changes to the surface topography such as fibrillation of the articular surface [37]. It therefore seems likely that an increase in cartilage friction following injury may cause excessive tissue shear deformation during joint movement and thus promote catabolic pathways in chondrocytes, ultimately leading to the development of degenerative conditions such as OA. To address this hypothesis, we developed a cytocompatible hydrogel system which allows for targeted changes to its surface friction without affecting other bulk physicochemical characteristics. We further

employed this system to study the biological response of hydrogel-encapsulated articular chondrocytes to shear loading to establish, for the first time, a functional relationship between surface friction and cellular homeostasis in mechanically loaded tissues.

In order to approach the low friction values characteristic for healthy articular cartilage, we incorporated SSA, a photocrosslinkable derivative of sulfonic acid which is anionic at physiological pH, into PEG-based hydrogels and co-polymerized these with cell-laden ALMA to form bilayered constructs. The presence of fixed negative charges in the surface layer was confirmed using EPIC-μCT (Fig. 2D) which indicated increasing charge densities from bilayered ALMA (high friction gels without SSA) to PEG-40S (moderate friction with 40 mol% SSA) and PEG-80S (low friction with 80 mol% SSA) hydrogel constructs. The negative charge densities of the surface hydrogel layer inversely correlated with the construct COFs (Fig. 2A), suggesting that covalent SSA incorporation reduced the surface friction of bilayered hydrogels. While the exact lubrication mechanisms were not investigated it this study, it is likely that incorporation of negative charge facilitated by SSA increased the electrostatic repulsion between the polyanionic gel and the stainless steel bioreactor loading platen, in turn resulting in reduced COFs [7]. Using this approach, we were able to tailor construct COFs without significantly affecting the bulk compressive moduli (Fig. 2B), mass swelling ratio, or water content (Fig. 2C) of bilayered constructs. We observed COFs of ~ 0.045 for PEG-80S constructs which approximate to COFs of healthy cartilage-on-cartilage (0.001 – 0.025) [26–29], while PEG-40S and ALMA constructs exhibited significantly higher COFs ranging from ~ 0.085 to ~ 0.092, and ~ 0.155 to ~ 0.170, respectively (Fig. 2A). These values correspond to kinetic COFs of articular cartilage affected by moderate to severe OA (stage 3–4) [27, 46, 47]. However, it has to be considered that the COF values of hydrogels and cartilage specimens depend on a variety of parameters including the sample geometry, applied normal force, sliding velocity, lubricant used, and the properties of the opposing surface. It is hence likely that reported COFs of healthy and diseased cartilage may vary from the COFs in vivo. Similarly, variations in the COFs determined in friction tests and the bioreactor used in this study may exist. In order to minimize these discrepancies, the tribometer was designed to permit measurement of hydrogel COFs against the loading platen used in the bioreactor with cell culture media as lubricant, hence replicating the loading and lubricant conditions employed in short- and long-term mechanical stimulation experiments. In diarthrodial joints, lubrication is provided by synovial fluid [60]. Since the experiments in this study involved the culture of hydrogel-encapsulated chondrocytes [61], the choice of lubricant was limited to a suitable cell culture media. Although differences in the lubrication efficacy of media and synovial fluid are expected, it was previously shown that testing using various lubricants yields fundamentally the same relationships between samples of varying surface properties [62], while the absolute COF values may differ between lubricant systems [53]. Accordingly, it is expected that the differences in frictional properties between ALMA, PEG-40S, and PEG-80S constructs are preserved when tested using other lubricants than culture media.

Limiting SSA incorporation to a thin surface layer allowed us to control hydrogel surface properties without influencing the microenvironment of cells encapsulated in ALMA, hence enabling the attribution of cell responses to mechanical loading to the frictional properties of the construct rather than differences in cell-matrix interactions. Employing a hydrogel-based

method also had significant advantages over alternative 3D models, such as cartilage explant cultures, which do not allow for precise tailoring of the COF or other physicochemical properties. In addition, if variations in explant surface friction occur, these are typically linked to differences in ECM structure and composition [33] which were shown to affect the chondrocyte phenotype through signalling mediated by cell-ECM interactions [63], making it challenging to isolate the effects of the explant's frictional properties on the observed cell behaviour following mechanical loading.

We hypothesized that articular cartilage surface friction and mechanical properties are intrinsically linked to chondrocyte homeostasis by governing the magnitude of tissue shear during normal joint ambulation. After establishing a means to control the frictional properties of hydrogels, we thus investigated the deformation of these constructs in response to mechanical loading replicating the sliding shear motion of articulating joints. As expected, we found that shear strain throughout the cell-containing hydrogel layer increased substantially with construct COFs, effectively mimicking the changes in cartilage biomechanics after injury and in the early stages of OA [36, 37]. Similar to the native tissue [36, 37], strain levels peaked in the superficial areas just below the variable friction hydrogel layer and dimished with depth (Fig. 2F, G). The magnitude of shear strain in low friction PEG-80S constructs (~2 – 4%) was consistent with previously reported strain levels for healthy cartilage-on-cartilage lubricated with synovial fluid, while strains in PEG-40S and ALMA were substantially higher as in fibrilated and osteoarthritic cartilage, ranging from ~6 – 13% and ~8 – 17%, respectively [36, 37]. However, given the complexity of biomechanical stimuli arising from a normal joint usage, shear strains *in vivo* may vary from these values which were obtained in uniaxial shear tests under static compression [36, 37], similar to the loading regimes applied in the present study. While this is a simplification of physiological loading conditions [64], previous studies indicated that the frictional properties of articular cartilage remain similar irrespective of whether compression is applied dynamically or statically [65], suggesting that the influence of cyclic compression on the magnitude of tissue/hydrogel shear strains may also be minor.

It was previously reported that excessive mechanical strains in articular cartilage can result in cell death [66] and ECM damage [67], in turn further reducing the intrinsic capacity for tissue maintenance and repair. The results of our short-term study indicated that, in this model, mechanical loading did not impact cell viability (Fig. 3), although shear strains in dynamically stimulated PEG-40S and ALMA constructs substantially exceeded physiological levels (Fig. 2F, G) [36, 37]. This may be explained by the differences in ECM mechanical properties and thus the magnitude of strain-induced mechanical stresses between native human tissue (aggregate modulus of ~ 0.5 – 0.9 MPa [68], young's modulus of ~ 1.5 – 3 MPa, unpublished data) and hydrogel constructs (Fig. 2B). Contrary to our hypothesis, construct frictional properties had no significant effect on gene expression patterns after one hour of mechanical stimulation in this short-term study (Supplementary Fig. S1). This lack of discernable differences in cell response may be related to the short duration of static preculture before mechanical stimulation (7 days) which may not allow for sufficient formation of a functional pericellular matrix, one of the key transducer of chondrocyte mechanotransduction, causing chondrocytes to respond poorly or detrimentally to mechanical stimuli [42]. Further reinforcing this hypothesis, the results from our long-term

gene expression study indicated a much more distinct transcriptional response of chondrocytes to dynamic shear following 21 days of preculture which was additionally highly dependent on construct surface friction. We found that expression of chondrogenic marker genes *COL2A1* (Fig. 5B) and *PRG4* (Fig. 5C) was significantly up-regulated in dynamically stimulated PEG-80S low friction constructs when compared to static controls, as well as high (ALMA) and moderate friction (PEG-40S) constructs. On the other hand, expression of chondrogenic marker genes remained at control level in shear-stimulated ALMA constructs, while *MMP3* expression was significantly increased (Fig. 5E). The protease MMP3 is a key mediator of cartilage degradation and has been found to be highly expressed in OA with protein levels correlating to OA severity [69]. These results hence indicate that the low level shear strains in PEG-80S induced transcription of chondrogenic genes, while constructs with higher COFs (Fig. 2A) and thus shear strains (Fig. 2F, G) amplified catabolic pathways in chondrocytes. Gene expression data were further confirmed on protein level using immunofluorescence staining techniques which revealed that the synthesis and accumulation of collagen type II was strongly dependent on the surface friction of mechanically stimulated constructs. Visual and statistical analysis revealed significantly higher amounts of accumulated collagen II in shear-stimulated PEG-80S when compared to static controls and other construct types (Fig. 5G–L, T), while accumulation in loaded ALMA constructs was decreased compared to unstimulated controls. These findings are in line with previous studies which indicated that minor dynamic shear strains, as they occur in PEG-80S constructs, produced constructs with 40 % more collagen, 25 % more proteoglycan, and 6-fold higher equilibrium modulus [31]. High shear strains, as in mechanically stimulated ALMA constructs, however, inhibited macromolecule synthesis [31].

In this study, chondrocytes were isolated from regions of macroscopically normal cartilage which was obtained from donors undergoing total knee arthroplasties for OA. While we cannot rule out that the phenotype of these cells differs from healthy chondrocytes of younger individuals, we have no reason to believe that chondrocytes from non-OA sources would show different responses to the loading conditions used in our study. During OA as well as propagation on tissue culture plastics, chondrocytes undergo dedifferentiation; a process characterized by an increase in the expression of collagen I and MMPs, and reduced expression of cartilage-specific markers such as collagen II and aggrecan [70–72]. Yet, the low cellularity of cartilage frequently renders monolayer expansion unavoidable in order to obtain sufficient cell numbers for clinical applications such as autologous chondrocyte implantation [73], as well as investigations in vitro. However, chondrocyte dedifferentiation can be reversed by cultivation in suitable 3D matrices under chondrogenic conditions [74]. Accordingly, isolated chondrocytes were expanded to passage 2 in order to obtain sufficient cell numbers for the bioreactor experiments and encapsulated in ALMA hydrogels [39]. Under such conditions, osteoarthritic and monolayer-expanded chondrocytes regain their ability to express cartilage-specific markers [39, 74, 75] and react to mechanical stimuli similar to cells from normal human [42] or animal cartilage [76]. Moreover, the use of chondrocytes derived from elderly human donors with OA in cartilage research is appropriate and important as this population is most likely to benefit from any improvement in our understanding of chondrocyte behaviour.

Previous studies suggested that intermittent compressive stimulation of tissue-engineered cartilage at low and moderate strain levels increased ECM molecule synthesis and resulted in higher mechanical properties [76, 77]. Similar to our earlier work utilizing ALMA as redifferentiation platform for chondrocytes [39], all construct types, independent of the composition of the surface hydrogel layer, were softer on day 32 compared to day 1 of culture (compare Fig. 2B and Fig. 4H). This is likely to be attributed to the hydrolytic [78] or non-specific enzymatic degradation [79] of ester bonds formed by the methacrylation of alginate hydroxyl groups [40]. However, dynamic shear loading partially reversed the decrease in construct stiffness, resulting in higher compressive moduli of shear stimulated ALMA and PEG-80S constructs when compared to static controls cultured for the same period of time (Fig. 4H). The increase in stiffness was the greatest for PEG-80S constructs (~ 2.5-fold increase over SC for PEG-80S; $p = 0.029$, versus ~ 1.9-fold increase for ALMA; $p = 0.036$) (Fig. 4H) which may be partially explained by the significantly higher accumulation of GAGs (Fig. 4G) and ECM molecules (Fig. 5) in these constructs following mechanical stimulation. In line with the gene expression and immunofluorescence analysis, GAG/DNA levels in shear-stimulated ALMA and PEG-40S constructs were similar to static control levels, indicating that the high magnitude shear strain impaired the chondrogenic capacity of encapsulated chondrocytes when compared to constructs with lower COFs.

5. Conclusion

In this study, we developed a cytocompatible hydrogel system which allows for targeted changes to its frictional properties without affecting other bulk physicochemical characteristics. The system is versatile and can be readily adapted to accommodate a variety of cell types, as well as hydrogel and scaffold materials, and can be employed to study the effects of variations in surface friction on cellular behaviour in response to physiologically relevant mechanical loading. We tested the applicability of the model in studying the response of human articular chondrocytes to shear loading and demonstrate that cartilage lubrication and surface friction may regulate chondrocyte homeostasis by governing the magnitude of tissue shear deformation during joint articulation. Our results indicate that dynamic shear stimulation of constructs with low surface friction causes low magnitude shear strains which significantly promote chondrogenesis and extracellular matrix synthesis as assessed by gene expression, immunofluorescence, and biochemical analysis. In contrast, shear stimulation of constructs with high surface friction can lead to excessive strains which impair chondrogenesis, but induce transcription of matrix metalloproteinases involved in the degradation of cartilage extracellular matrix in osteoarthritis. Based on these findings, we propose that changes in cartilage lubrication and frictional properties as they occur after traumatic joint injury [32–35] may be involved in the initiation of posttraumatic cartilage degeneration by increasing mechanical strains within the tissue beyond a physiological level, causing inhibition of cartilaginous matrix synthesis and activation of catabolic pathways.

Supplementary Material

Refer to Web version on PubMed Central for supplementary material.

Acknowledgments

The authors would like to thank the Australian Research Council (DP110103543, FT110100166) and National Institutes of Health (P01 AG007996) for funding. Also, we would like to thank Carly Sutton for help with the design and manufacturing of the custom bioreactor components, as well as Ben Gillen and Ewa Gillen for the production of the computer animation illustrating the working principle of the shear stimulation bioreactor.

References

1. Elisseeff J. Hydrogels: structure starts to gel. Nature materials. 2008; 7(4):271–273. [PubMed: 18354410]
2. Malda J, Visser J, Melchels FP, Jungst T, Hennink WE, Dhert WJ, Groll J, Hutmacher DW. 25th anniversary article: Engineering hydrogels for biofabrication. Advanced materials. 2013; 25(36): 5011–5028. [PubMed: 24038336]
3. Klein TJ, Rizzi SC, Reichert JC, Georgi N, Malda J, Schuurman W, Crawford RW, Hutmacher DW. Strategies for zonal cartilage repair using hydrogels. Macromolecular bioscience. 2009; 9(11):1049–1058. [PubMed: 19739068]
4. Loessner D, Meinert C, Kaemmerer E, Martine LC, Yue K, Levett PA, Klein TJ, Melchels FP, Khademhosseini A, Hutmacher DW. Functionalization, preparation and use of cell-laden gelatin methacryloyl-based hydrogels as modular tissue culture platforms. Nature protocols. 2016; 11(4): 727–746. [PubMed: 26985572]
5. Schuurman W, Levett PA, Pot MW, van Weeren PR, Dhert WJ, Hutmacher DW, Melchels FP, Klein TJ, Malda J. Gelatin-methacrylamide hydrogels as potential biomaterials for fabrication of tissue-engineered cartilage constructs. Macromolecular bioscience. 2013; 13(5):551–561. [PubMed: 23420700]
6. Levett PA, Melchels FP, Schrobback K, Hutmacher DW, Malda J, Klein TJ. A biomimetic extracellular matrix for cartilage tissue engineering centered on photocurable gelatin, hyaluronic acid and chondroitin sulfate. Acta biomaterialia. 2014; 10(1):214–223. [PubMed: 24140603]
7. Gong JP. Friction and lubrication of hydrogels—its richness and complexity. Soft matter. 2006; 2(7): 544–552.
8. Hutmacher DW. Biomaterials offer cancer research the third dimension. Nature materials. 2010; 9(2):90–93. [PubMed: 20094076]
9. Ahmed EM. Hydrogel: Preparation, characterization, and applications: A review. J Adv Res. 2015; 6(2):105–121. [PubMed: 25750745]
10. Pathak A, Kumar S. Independent regulation of tumor cell migration by matrix stiffness and confinement. Proceedings of the National Academy of Sciences of the United States of America. 2012; 109(26):10334–10339. [PubMed: 22689955]
11. Engler AJ, Sen S, Sweeney HL, Discher DE. Matrix elasticity directs stem cell lineage specification. Cell. 2006; 126(4):677–689. [PubMed: 16923388]
12. Keung AJ, de Juan-Pardo EM, Schaffer DV, Kumar S. Rho GTPases mediate the mechanosensitive lineage commitment of neural stem cells. Stem Cells. 2011; 29(11):1886–1897. [PubMed: 21956892]
13. Huebsch N, Lippens E, Lee K, Mehta M, Koshy ST, Darnell MC, Desai RM, Madl CM, Xu M, Zhao X, Chaudhuri O, Verbeke C, Kim WS, Alim K, Mammoto A, Ingber DE, Duda GN, Mooney DJ. Matrix elasticity of void-forming hydrogels controls transplanted-stem-cell-mediated bone formation. Nature materials. 2015; 14(12):1269–1277. [PubMed: 26366848]
14. Paszek MJ, Zahir N, Johnson KR, Lakins JN, Rozenberg GI, Gefen A, Reinhart-King CA, Margulies SS, Dembo M, Boettiger D, Hammer DA, Weaver VM. Tensional homeostasis and the malignant phenotype. Cancer Cell. 2005; 8(3):241–254. [PubMed: 16169468]
15. Caiazzo M, Okawa Y, Ranga A, Piersigilli A, Tabata Y, Lutolf MP. Defined three-dimensional microenvironments boost induction of pluripotency. Nature materials. 2016; 15(3):344–352. [PubMed: 26752655]
16. Chen CS. Mechanotransduction - a field pulling together? Journal of cell science. 2008; 121(Pt 20):3285–3292. [PubMed: 18843115]

17. Buschmann MD, Gluzband YA, Grodzinsky AJ, Hunziker EB. Mechanical compression modulates matrix biosynthesis in chondrocyte/agarose culture. Journal of cell science. 1995; 108(Pt 4):1497–1508. [PubMed: 7615670]
18. Blain EJ. Mechanical regulation of matrix metalloproteinases. Front Biosci. 2007; 12:507–527. [PubMed: 17127313]
19. Carter DR, Beaupre GS, Wong M, Smith RL, Andriacchi TP, Schurman DJ. The mechanobiology of articular cartilage development and degeneration. Clinical orthopaedics and related research. 2004; (427 Suppl):S69–S77. [PubMed: 15480079]
20. Beaupre GS, Stevens SS, Carter DR. Mechanobiology in the development, maintenance, and degeneration of articular cartilage. Journal of rehabilitation research and development. 2000; 37(2):145–151. [PubMed: 10850820]
21. Lewis PR, McCutchen CW. Experimental evidence for weeping lubrication in mammalian joints. Nature. 1959; 184:1285. [PubMed: 14416552]
22. Dowson D, Jin ZM. Micro-elastohydrodynamic lubrication of synovial joints. Engineering in medicine. 1986; 15(2):63–65. [PubMed: 3709914]
23. Schmidt TA, Gastelum NS, Nguyen QT, Schumacher BL, Sah RL. Boundary lubrication of articular cartilage: role of synovial fluid constituents. Arthritis and rheumatism. 2007; 56(3):882–891. [PubMed: 17328061]
24. Hou JS, Mow VC, Lai WM, Holmes MH. An analysis of the squeeze-film lubrication mechanism for articular cartilage. Journal of biomechanics. 1992; 25(3):247–259. [PubMed: 1564060]
25. Ateshian GA. The role of interstitial fluid pressurization in articular cartilage lubrication. Journal of biomechanics. 2009; 42(9):1163–1176. [PubMed: 19464689]
26. Athanasiou, KA., Darling, EM., Hu, JC. Articular Cartilage Tissue Engineering. San Rafael, CA: Morgan & Claypool; 2009.
27. Singh A, Corvelli M, Unterman SA, Wepasnick KA, McDonnell P, Elisseeff JH. Enhanced lubrication on tissue and biomaterial surfaces through peptide-mediated binding of hyaluronic acid. Nature materials. 2014; 13(10):988–995. [PubMed: 25087069]
28. Caligaris M, Ateshian GA. Effects of sustained interstitial fluid pressurization under migrating contact area, and boundary lubrication by synovial fluid, on cartilage friction. Osteoarthritis and cartilage/OARS, Osteoarthritis Research Society. 2008; 16(10):1220–1227.
29. Li F, Su Y, Wang J, Wu G, Wang C. Influence of dynamic load on friction behavior of human articular cartilage, stainless steel and polyvinyl alcohol hydrogel as artificial cartilage. Journal of materials science. Materials in medicine. 2010; 21(1):147–154. [PubMed: 19756967]
30. Jin M, Frank EH, Quinn TM, Hunziker EB, Grodzinsky AJ. Tissue shear deformation stimulates proteoglycan and protein biosynthesis in bovine cartilage explants. Archives of biochemistry and biophysics. 2001; 395(1):41–48. [PubMed: 11673864]
31. Waldman SD, Spiteri CG, Grynpas MD, Pilliar RM, Kandel RA. Long-term intermittent shear deformation improves the quality of cartilaginous tissue formed in vitro. Journal of orthopaedic research : official publication of the Orthopaedic Research Society. 2003; 21(4):590–596. [PubMed: 12798056]
32. Elsaid KA, Jay GD, Warman ML, Rhee DK, Chichester CO. Association of articular cartilage degradation and loss of boundary-lubricating ability of synovial fluid following injury and inflammatory arthritis. Arthritis and rheumatism. 2005; 52(6):1746–1755. [PubMed: 15934070]
33. Teeple E, Elsaid KA, Fleming BC, Jay GD, Aslani K, Crisco JJ, Mechrefe AP. Coefficients of friction, lubricin, and cartilage damage in the anterior cruciate ligament-deficient guinea pig knee. Journal of orthopaedic research : official publication of the Orthopaedic Research Society. 2008; 26(2):231–237. [PubMed: 17868097]
34. Coles JM, Zhang L, Blum JJ, Warman ML, Jay GD, Guilak F, Zauscher S. Loss of cartilage structure, stiffness, and frictional properties in mice lacking PRG4. Arthritis and rheumatism. 2010; 62(6):1666–1674. [PubMed: 20191580]
35. Roos EM. Joint injury causes knee osteoarthritis in young adults. Current opinion in rheumatology. 2005; 17(2):195–200. [PubMed: 15711235]

36. Wong BL, Bae WC, Chun J, Gratz KR, Lotz M, Sah RL. Biomechanics of cartilage articulation: effects of lubrication and degeneration on shear deformation. Arthritis and rheumatism. 2008; 58(7):2065–2074. [PubMed: 18576324]
37. Wong BL, Bae WC, Gratz KR, Sah RL. Shear deformation kinematics during cartilage articulation: effect of lubrication, degeneration, and stress relaxation. Molecular & cellular biomechanics : MCB. 2008; 5(3):197–206. [PubMed: 18751528]
38. Wong BL, Kim SH, Antonacci JM, McIlwraith CW, Sah RL. Cartilage shear dynamics during tibio-femoral articulation: effect of acute joint injury and tribosupplementation on synovial fluid lubrication. Osteoarthritis and cartilage/OARS, Osteoarthritis Research Society. 2010; 18(3):464–471.
39. Levett PA, Melchels FP, Schrobback K, Hutmacher DW, Malda J, Klein TJ. Chondrocyte redifferentiation and construct mechanical property development in single-component photocrosslinkable hydrogels. Journal of biomedical materials research. Part A. 2014; 102(8): 2544–2553. [PubMed: 24000167]
40. Smeds KA, Pfister-Serres A, Miki D, Dastgheib K, Inoue M, Hatchell DL, Grinstaff MW. Photocrosslinkable polysaccharides for in situ hydrogel formation. Journal of biomedical materials research. 2001; 54(1):115–121. [PubMed: 11077410]
41. Klein TJ, Rizzi SC, Schrobback K, Reichert JC, Jeon JE, Crawford RW, Hutmacher DW. Long-term effects of hydrogel properties on human chondrocyte behavior Soft matter. 2010; 6(20):5175–5183.
42. Jeon JE, Schrobback K, Meinert C, Sramek V, Hutmacher DW, Klein TJ. Effect of preculture and loading on expression of matrix molecules, matrix metalloproteinases, and cytokines by expanded osteoarthritic chondrocytes. Arthritis and rheumatism. 2013; 65(9):2356–2367. [PubMed: 23780780]
43. Palmer AW, Guldberg RE, Levenston ME. Analysis of cartilage matrix fixed charge density and three-dimensional morphology via contrast-enhanced microcomputed tomography. Proceedings of the National Academy of Sciences of the United States of America. 2006; 103(51):19255–19260. [PubMed: 17158799]
44. Schrobback K, Malda J, Crawford RW, Upton Z, Leavesley DI, Klein TJ. Effects of oxygen on zonal marker expression in human articular chondrocytes. Tissue engineering. Part A. 2012; 18(9–10):920–933. [PubMed: 22097912]
45. Schrobback K, Wrobel J, Hutmacher DW, Woodfield TB, Klein TJ. Stage-specific embryonic antigen-4 is not a marker for chondrogenic and osteogenic potential in cultured chondrocytes and mesenchymal progenitor cells. Tissue engineering. Part A. 2013; 19(11–12):1316–1326. [PubMed: 23301556]
46. Neu CP, Reddi AH, Komvopoulos K, Schmid TM, Di Cesare PE. Increased friction coefficient and superficial zone protein expression in patients with advanced osteoarthritis. Arthritis and rheumatism. 2010; 62(9):2680–2687. [PubMed: 20499384]
47. Young AA, McLennan S, Smith MM, Smith SM, Cake MA, Read RA, Melrose J, Sonnabend DH, Flannery CR, Little CB. Proteoglycan 4 downregulation in a sheep meniscectomy model of early osteoarthritis. Arthritis Res Ther. 2006; 8(2):R41. [PubMed: 16469119]
48. Benya PD, Shaffer JD. Dedifferentiated chondrocytes reexpress the differentiated collagen phenotype when cultured in agarose gels. Cell. 1982; 30(1):215–224. [PubMed: 7127471]
49. Watanabe H, Yamada Y, Kimata K. Roles of aggrecan, a large chondroitin sulfate proteoglycan, in cartilage structure and function. Journal of biochemistry. 1998; 124(4):687–693. [PubMed: 9756610]
50. Schumacher BL, Block JA, Schmid TM, Aydelotte MB, Kuettner KE. A novel proteoglycan synthesized and secreted by chondrocytes of the superficial zone of articular cartilage. Archives of biochemistry and biophysics. 1994; 311(1):144–152. [PubMed: 8185311]
51. Sivan S, Schroeder A, Verberne G, Merkher Y, Diminsky D, Priev A, Maroudas A, Halperin G, Nitzan D, Etsion I, Barenholz Y. Liposomes act as effective biolubricants for friction reduction in human synovial joints. Langmuir : the ACS journal of surfaces and colloids. 2010; 26(2):1107–1116. [PubMed: 20014818]

52. Daniel M. Boundary cartilage lubrication: review of current concepts. Wien Med Wochenschr. 2014; 164(5–6):88–94. [PubMed: 24081750]

53. Caligaris M, Canal CE, Ahmad CS, Gardner TR, Ateshian GA. Investigation of the frictional response of osteoarthritic human tibiofemoral joints and the potential beneficial tribological effect of healthy synovial fluid. Osteoarthritis and cartilage/OARS, Osteoarthritis Research Society. 2009; 17(10):1327–1332.

54. Jay GD, Elsaid KA, Zack J, Robinson K, Trespalacios F, Cha CJ, Chichester CO. Lubricating ability of aspirated synovial fluid from emergency department patients with knee joint synovitis. J Rheumatol. 2004; 31(3):557–564. [PubMed: 14994405]

55. Morrell KC, Hodge WA, Krebs DE, Mann RW. Corroboration of in vivo cartilage pressures with implications for synovial joint tribology and osteoarthritis causation. Proceedings of the National Academy of Sciences of the United States of America. 2005; 102(41):14819–14824. [PubMed: 16203974]

56. Batiste DL, Kirkley A, Laverty S, Thain LM, Spouge AR, Holdsworth DW. Ex vivo characterization of articular cartilage and bone lesions in a rabbit ACL transection model of osteoarthritis using MRI and micro-CT. Osteoarthritis and cartilage/OARS, Osteoarthritis Research Society. 2004; 12(12):986–996.

57. Stoop R, Buma P, van der Kraan PM, Hollander AP, Billinghurst RC, Meijers TH, Poole AR, van den Berg WB. Type II collagen degradation in articular cartilage fibrillation after anterior cruciate ligament transection in rats. Osteoarthritis and cartilage/OARS, Osteoarthritis Research Society. 2001; 9(4):308–315.

58. Lee SS, Duong CT, Park SH, Cho Y, Park S, Park S. Frictional response of normal and osteoarthritic articular cartilage in human femoral head. Proceedings of the Institution of Mechanical Engineers. Part H, Journal of engineering in medicine. 2013; 227(2):129–137.

59. Desrochers J, Amrein MW, Matyas JR. Microscale surface friction of articular cartilage in early osteoarthritis. J Mech Behav Biomed Mater. 2013; 25:11–22. [PubMed: 23726921]

60. McNary SM, Athanasiou KA, Reddi AH. Engineering lubrication in articular cartilage. Tissue engineering. Part B, Reviews. 2012; 18(2):88–100. [PubMed: 21955119]

61. Caron MM, Emans PJ, Coolsen MM, Voss L, Surtel DA, Cremers A, van Rhijn LW, Welting TJ. Redifferentiation of dedifferentiated human articular chondrocytes: comparison of 2D and 3D cultures. Osteoarthritis and cartilage/OARS, Osteoarthritis Research Society. 2012; 20(10):1170–1178.

62. Forster H, Fisher J. The influence of loading time and lubricant on the friction of articular cartilage. Proceedings of the Institution of Mechanical Engineers. Part H, Journal of engineering in medicine. 1996; 210(2):109–119.

63. Grogan SP, Chen X, Sovani S, Taniguchi N, Colwell CW Jr, Lotz MK, D'Lima DD. Influence of cartilage extracellular matrix molecules on cell phenotype and neocartilage formation. Tissue engineering. Part A. 2014; 20(1–2):264–274. [PubMed: 23962090]

64. Halonen KS, Mononen ME, Jurvelin JS, Toyras J, Korhonen RK. Importance of depth-wise distribution of collagen and proteoglycans in articular cartilage--a 3D finite element study of stresses and strains in human knee joint. Journal of biomechanics. 2013; 46(6):1184–1192. [PubMed: 23384762]

65. Krishnan R, Mariner EN, Ateshian GA. Effect of dynamic loading on the frictional response of bovine articular cartilage. Journal of biomechanics. 2005; 38(8):1665–1673. [PubMed: 15958224]

66. Loening AM, James IE, Levenston ME, Badger AM, Frank EH, Kurz B, Nuttall ME, Hung HH, Blake SM, Grodzinsky AJ, Lark MW. Injurious mechanical compression of bovine articular cartilage induces chondrocyte apoptosis. Archives of biochemistry and biophysics. 2000; 381(2): 205–212. [PubMed: 11032407]

67. Thibault M, Poole AR, Buschmann MD. Cyclic compression of cartilage/bone explants in vitro leads to physical weakening, mechanical breakdown of collagen and release of matrix fragments. Journal of orthopaedic research : official publication of the Orthopaedic Research Society. 2002; 20(6):1265–1273. [PubMed: 12472239]

68. Athanasiou KA, Rosenwasser MP, Buckwalter JA, Malinin TI, Mow VC. Interspecies comparisons of in situ intrinsic mechanical properties of distal femoral cartilage. Journal of orthopaedic

research : official publication of the Orthopaedic Research Society. 1991; 9(3):330–340. [PubMed: 2010837]

69. Chen JJ, Huang JF, Du WX, Tong PJ. Expression and significance of MMP3 in synovium of knee joint at different stage in osteoarthritis patients. Asian Pac J Trop Med. 2014; 7(4):297–300. [PubMed: 24507680]
70. Poole AR, Kobayashi M, Yasuda T, Laverty S, Mwale F, Kojima T, Sakai T, Wahl C, El-Maadawy S, Webb G, Tchetina E, Wu W. Type II collagen degradation and its regulation in articular cartilage in osteoarthritis. Annals of the rheumatic diseases. 2002; 61(Suppl 2):ii78–ii81. [PubMed: 12379630]
71. Duan L, Ma B, Liang Y, Chen J, Zhu W, Li M, Wang D. Cytokine networking of chondrocyte dedifferentiation in vitro and its implications for cell-based cartilage therapy. American journal of translational research. 2015; 7(2):194–208. [PubMed: 25901191]
72. Schnabel M, Marlovits S, Eckhoff G, Fichtel I, Gotzen L, Vecsei V, Schlegel J. Dedifferentiation-associated changes in morphology and gene expression in primary human articular chondrocytes in cell culture. Osteoarthritis and cartilage/OARS, Osteoarthritis Research Society. 2002; 10(1): 62–70.
73. Makris EA, Gomoll AH, Malizos KN, Hu JC, Athanasiou KA. Repair and tissue engineering techniques for articular cartilage. Nature reviews. Rheumatology. 2015; 11(1):21–34. [PubMed: 25247412]
74. Hsieh-Bonassera ND, Wu I, Lin JK, Schumacher BL, Chen AC, Masuda K, Bugbee WD, Sah RL. Expansion and redifferentiation of chondrocytes from osteoarthritic cartilage: cells for human cartilage tissue engineering. Tissue engineering. Part A. 2009; 15(11):3513–3523. [PubMed: 19456239]
75. Dehne T, Karlsson C, Ringe J, Sittinger M, Lindahl A. Chondrogenic differentiation potential of osteoarthritic chondrocytes and their possible use in matrix-associated autologous chondrocyte transplantation. Arthritis Research & Therapy. 2009; 11(5):1–14.
76. Mauck RL, Soltz MA, Wang CC, Wong DD, Chao PH, Valhmu WB, Hung CT, Ateshian GA. Functional tissue engineering of articular cartilage through dynamic loading of chondrocyte-seeded agarose gels. Journal of biomechanical engineering. 2000; 122(3):252–260. [PubMed: 10923293]
77. Waldman SD, Spiteri CG, Grynpas MD, Pilliar RM, Kandel RA. Long-term intermittent compressive stimulation improves the composition and mechanical properties of tissue-engineered cartilage. Tissue engineering. 2004; 10(9–10):1323–1331. [PubMed: 15588393]
78. Li S. Hydrolytic degradation characteristics of aliphatic polyesters derived from lactic and glycolic acids. Journal of biomedical materials research. 1999; 48(3):342–353. [PubMed: 10398040]
79. Romano D, Bonomi F, de Mattos MC, de Sousa Fonseca T, de Oliveira MD, Molinari F. Esterases as stereoselective biocatalysts. Biotechnol Adv. 2015

Statement of significance

Excessive mechanical loading is believed to be a major risk factor inducing pathogenesis of articular cartilage and other load-bearing tissues. Yet, the mechanisms leading to increased transmission of mechanical stimuli to cells embedded in the tissue remain largely unexplored. Here, we demonstrate that the tribological properties of load-bearing tissues regulate cellular behaviour by governing the magnitude of mechanical deformation arising from physiological tissue function. Based on these findings, we propose that changes to articular surface friction as they occur with trauma, aging, or disease, may initiate tissue pathology by increasing the magnitude of mechanical stress on embedded cells beyond a physiological level.

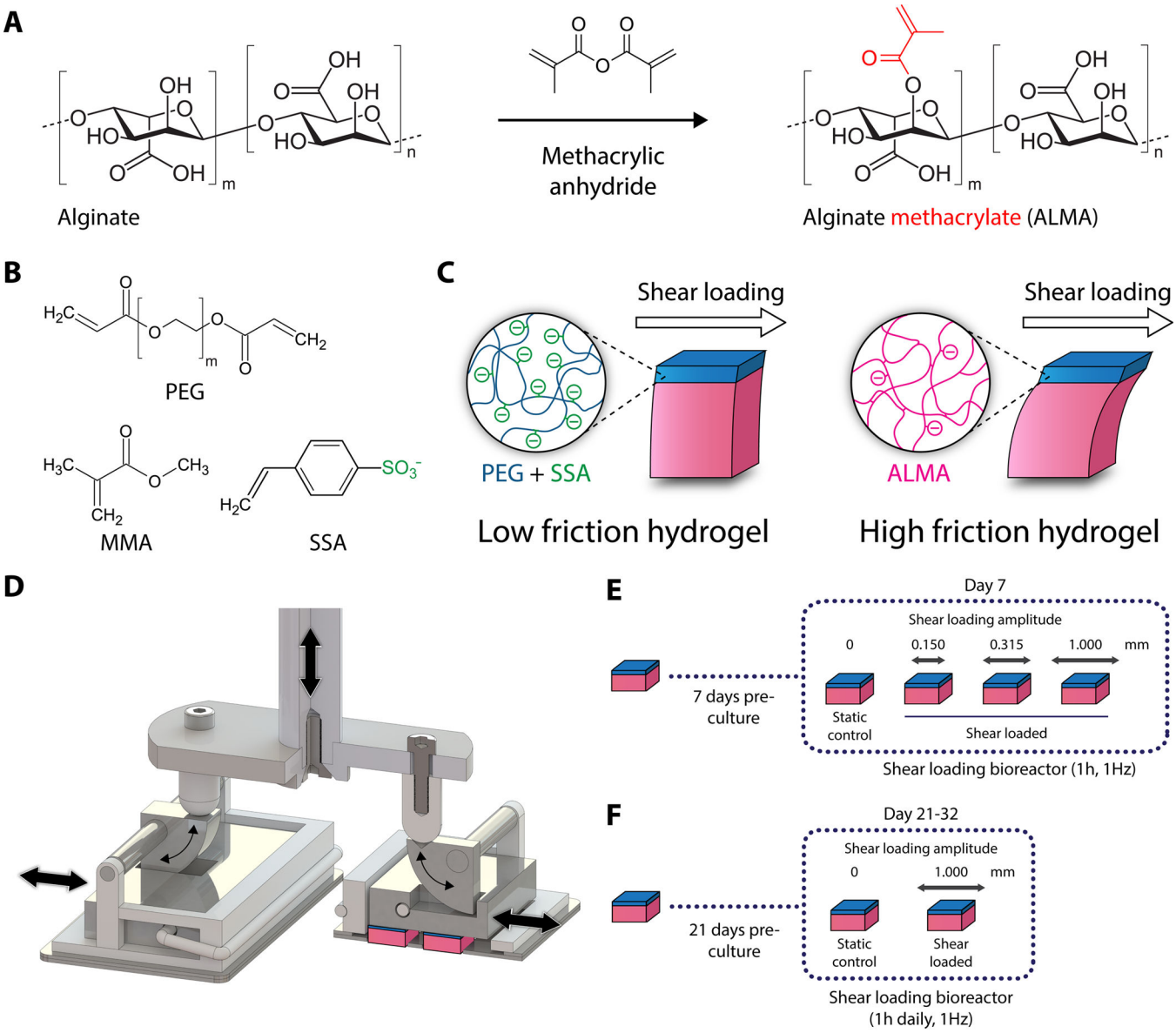

Figure 1.

Composition of bilayered hydrogel constructs with tailorable surface friction, schematic of the shear loading bioreactor and experimental overview. (A) Methacrylation of alginate, a natural hydrogel-forming polysaccharide commonly used for chondrocyte culture, enables cell-encapsulation by photopolymerization and improved control over construct mechanical properties. (B) To tailor frictional properties, synthetic hydrogels based on poly(ethylene glycol) diacrylate (PEG) were synthesized with varying concentrations of 4-styrene-sulfonic acid (SSA) and methyl methacrylate (MMA) and combined with cell-laden alginate methacrylate (ALMA) hydrogels to form bilayered constructs. (C) Schematic depicting shear deformation of low friction constructs containing high concentrations of negative charge facilitated by SSA and high friction constructs consisting of a cell-containing and a cell-free alginate methacrylate (ALMA) surface layer. (D) Rendered partial cross-section of

the custom shear loading bioreactor chamber exerting sliding shear motion to hydrogel constructs. (E) A short-term experiment for the optimisation of the shear loading amplitude was performed at 1 Hz for 1 h with either 0 mm, 0.15 mm, 0.315 mm, or 1 mm shear amplitude following 7 days of free-swelling preculture. (F) For long-term experiments, cell-hydrogel constructs were precultured for 21 days and subsequently shear loaded for 1 h daily over 11 days at 1 mm amplitude and a frequency of 1 Hz.

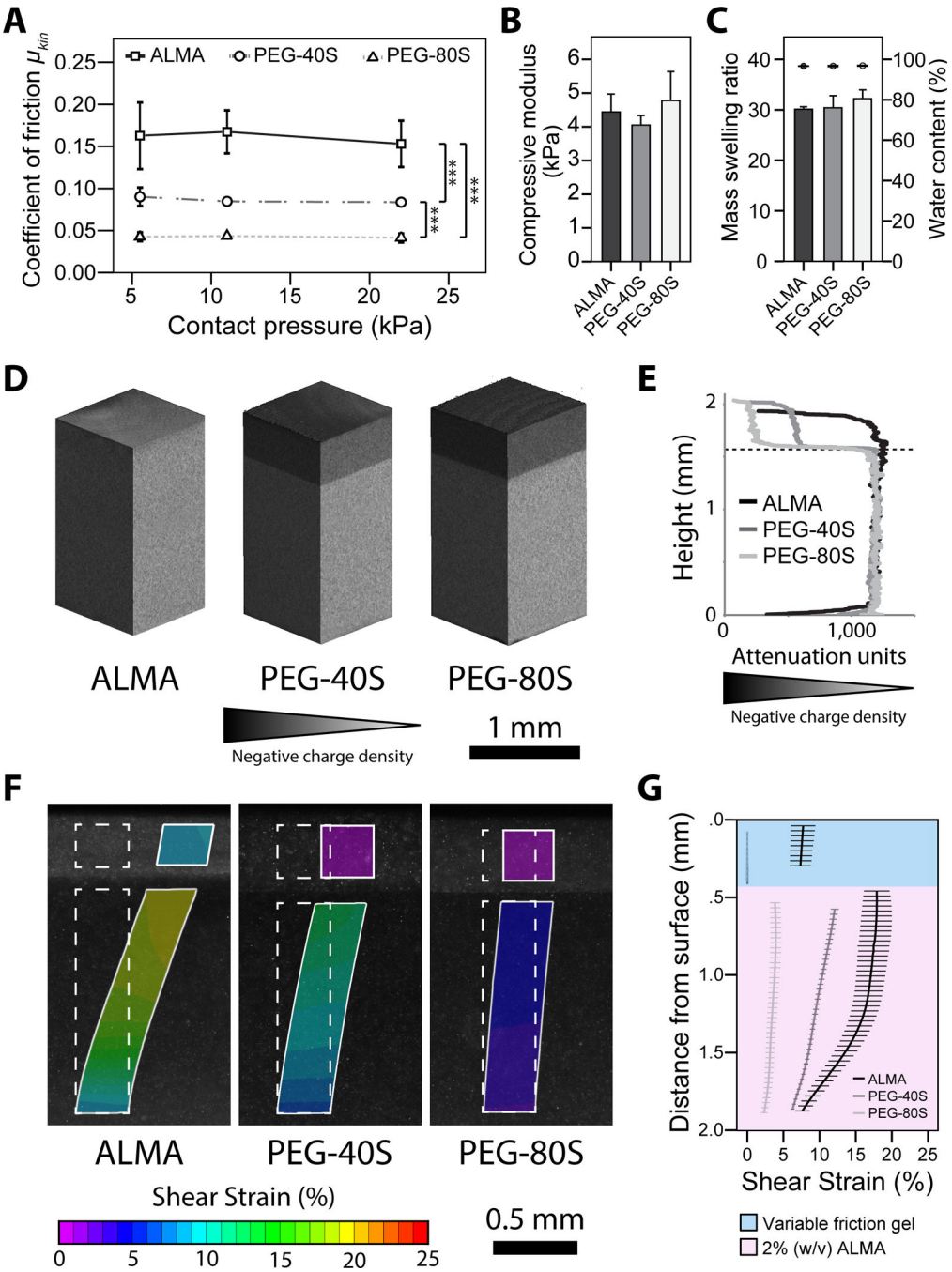

Figure 2.

Frictional and physicochemical properties of bilayered hydrogel constructs and their effect on hydrogel shear deformation. Bilayered ALMA, PEG-40S, and PEG-80S hydrogel constructs were analysed to determine their (A) dynamic coefficients of friction (mean ± SD, n = 5, *** = $p < 0.001$), (B) compressive moduli at day 1 (mean + SD, n = 3) and (C) mass swelling ratios (bars) as well as water contents (dots) of bilayered constructs (mean ± SD, n = 3). (D) Cross-sections and (E) quantified attenuation values from EPIC-μCT scans illustrating differences in surface hydrogel negative charge densities in bilayered constructs

(attenuation scales range from −5,000 (black) to 20,000 (white)). (F) Microscopic images of the peak shear strain in ALMA, PEG-40S, and PEG-80S hydrogel constructs in response to sliding shear motion and (G) depth-dependent changes in shear strains in the variable friction PEG gel and ALMA quantified using digital image correlation (mean ± SD, n = 2).

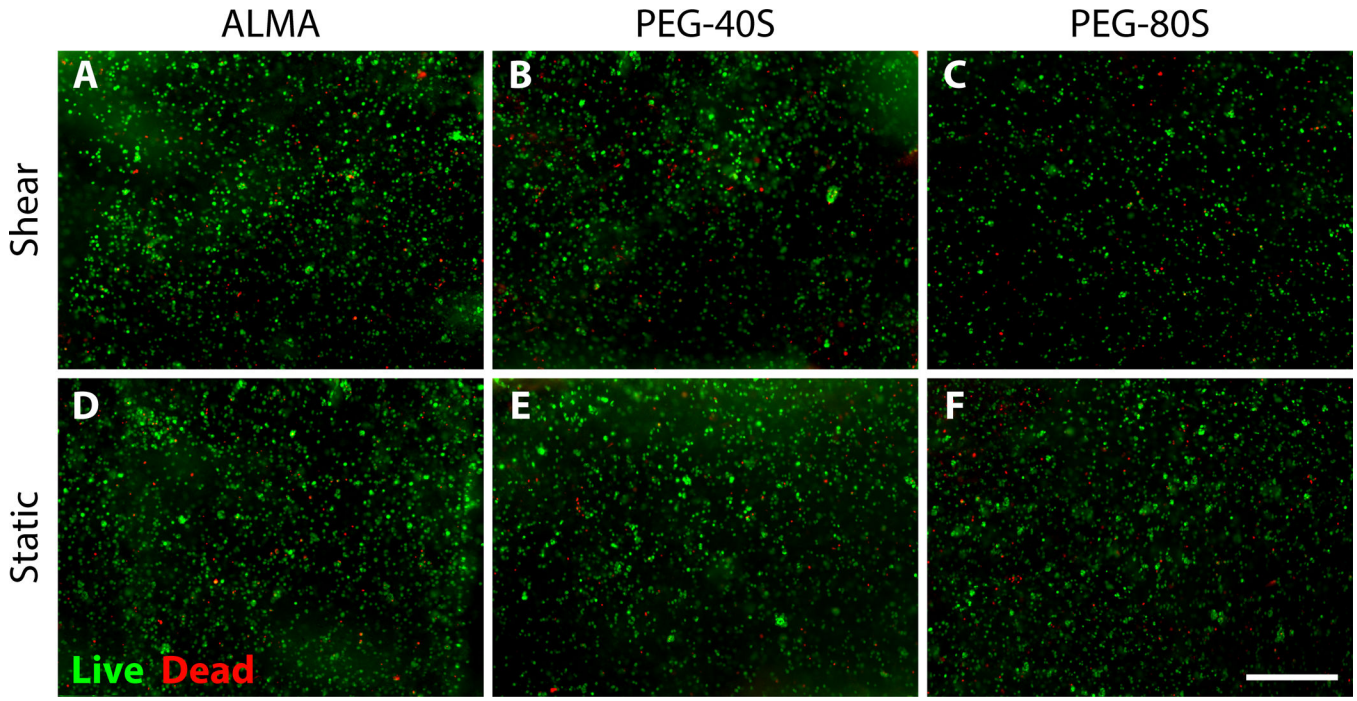

Figure 3.

Cell viability following short-term shear-stimulation of hydrogel constructs with variable surface friction. Viability of human articular chondrocytes in bilayered (A, D) ALMA, (B, E) PEG-40s, and (C, F) PEG-80S constructs (A–C) after dynamic shear stimulation and (D–F) in unstimulated controls. Living cells appear green and dead cells appear red. Scale bar: 500 μm.

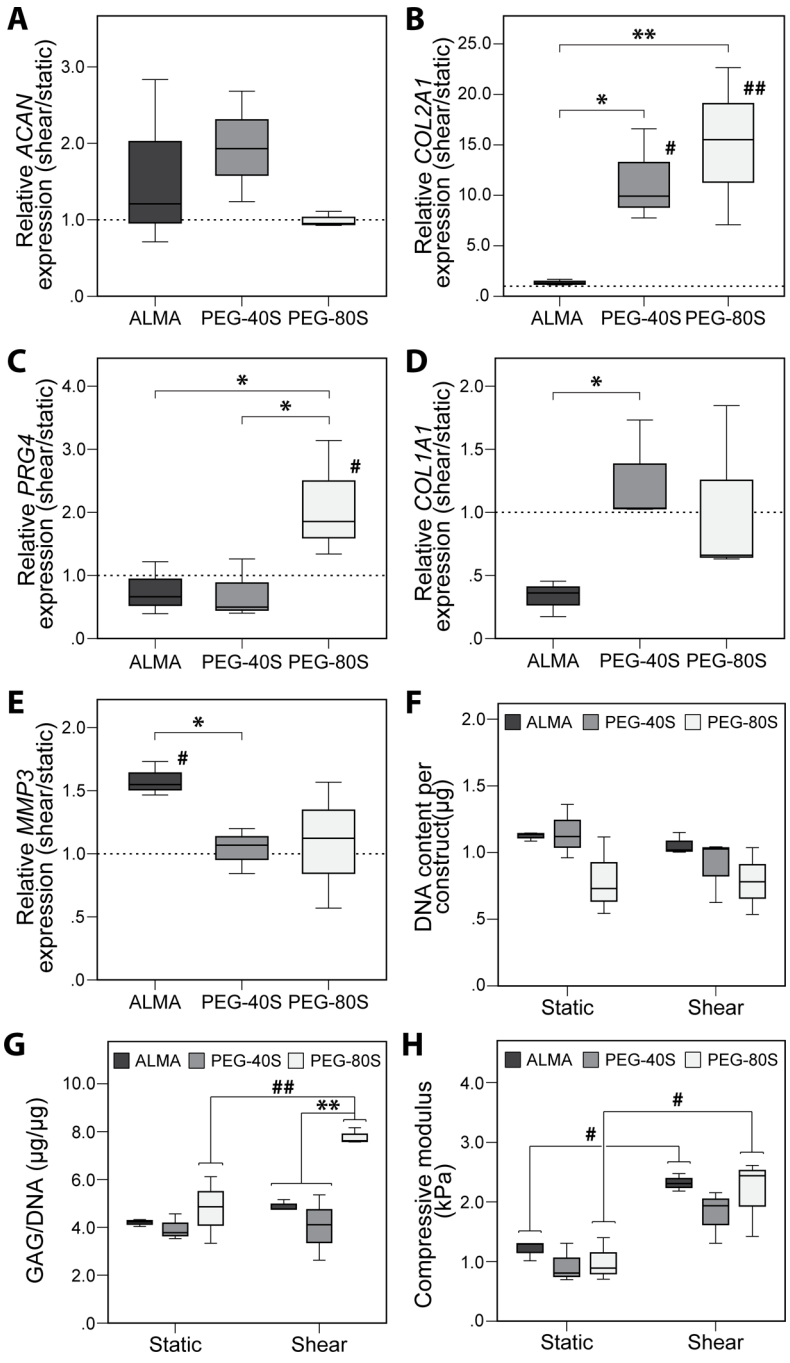

Figure 4.

Relative gene expression levels, biochemical and mechanical properties of hydrogel constructs with variable surface friction after long-term intermittent shear stimulation. Relative mRNA expression levels of (A) aggrecan, (B) collagen type II, (C) proteoglycan 4, (D) collagen type I, and (E) matrix metalloproteinase 3 of human articular chondrocytes embedded and shear-stimulated in ALMA, PEG-40S, and PEG-80S constructs. Gene expression of shear-stimulated constructs (shear) was normalized to static controls (static; mean relative expression indicated by broken line). (F) DNA content, (G) GAG retained in

constructs normalized to DNA content, and (H) compressive moduli of shear-stimulated and statically cultured ALMA, PEG-40S, and PEG-80S constructs. Significant differences between shear-stimulated constructs and static controls are indicated by # ($p < 0.05$) or ## ($p < 0.01$). Significant differences between constructs types are indicated by * ($p < 0.05$) or ** ($p < 0.01$) (n = 3).

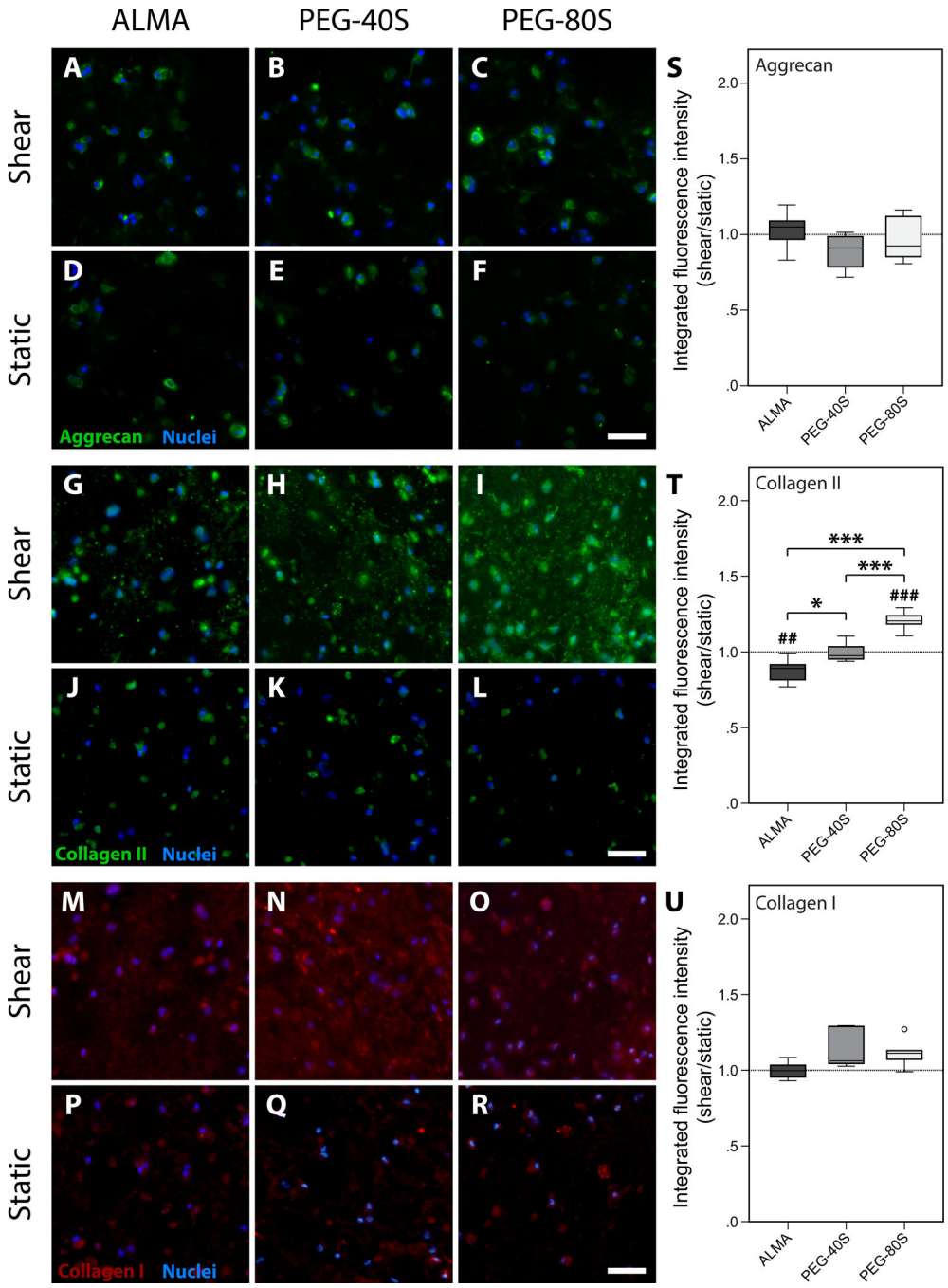

Figure 5.

Effect of long-term intermittent shear stimulation on extracellular matrix production in bilayered hydrogel constructs with varying frictional surface properties. Following a static preculture period of 21 days, ALMA, PEG-40S and PEG-80S hydrogels were (A–C, G–I, M–O) intermittently shear-stimulated or (D–F, J–L, P–R) statically cultured for another 11 days. Immunoreactive regions for aggrecan (A–F) and collagen type II (G–L) appear green, while immunoreactive regions for collagen type I (M–R) appear red. Nuclei were counterstained with DAPI (blue). Scale bars: 50 μm. Integrated fluorescence densities for (S)

aggrecan, (T) collagen type II, and (U) collagen type I stainings were normalized to DAPI intensities and expressed as the ratio of shear-stimulated to static control constructs. Significant differences in integrated staining intensities between shear-stimulated constructs and static controls are indicated by ## ($p < 0.01$) or ### ($p < 0.001$). Significant differences between construct types are indicated by * ($p < 0.05$), ** ($p < 0.01$) or *** ($p < 0.001$) (n = 6 images from 2 replicate samples).

Table 1

Composition of bilayered hydrogels with controlled surface friction

	Cell-free surface layer							
	PEG		SSA		MMA		ALMA	
Notation	% (w/v)	mol%	% (w/v)	mol%	% (w/v)	mol%	% (w/v)	Cell-laden layer
ALMA	0	0	0	0	0	0	2	2 % (w/v) ALMA
PEG-40S*	11.3	20	6.7	40	3.2	40	0	2 % (w/v) ALMA
PEG-80S*	11.3	20	13.3	80	0	0	0	2 % (w/v) ALMA

*Notations 40S and 80S refer to the percentage of SSA molecules to total hydrogel molarity (mol%)